

# Bayesian estimation for novel geometric INGARCH model

Divya Kuttenthalil Andrews<sup>a</sup>, N. Balakrishna<sup>a,b</sup>,

<sup>a</sup>*Cochin University of Science and Technology, Kochi, India.*

<sup>b</sup>*Indian Institute of Technology, Tirupati, India.*

---

## Abstract

This paper introduces an integer-valued generalized autoregressive conditional heteroskedasticity (INGARCH) model based on the novel geometric distribution and discusses some of its properties. The parameter estimation problem of the models are studied by conditional maximum likelihood and Bayesian approach using Hamiltonian Monte Carlo (HMC) algorithm. The results of the simulation studies and real data analysis affirm the good performance of the estimators and the model.

Keywords: Bayesian inference; Hamiltonian Monte Carlo; INGARCH; count time series.

---

## 1. Introduction

Count time series are often encountered in practical applications, particularly in fields such as insurance, healthcare, epidemiology, queuing models, communications, reliability studies, and meteorology. Examples of such counts include the number of patients, crime incidents, transmitted messages etc. Several models have been designed to analyze count time series, focusing on their marginal distributions and autocorrelation structures. These models are typically divided into two broad categories: models based on the 'thinning' operator and those of the regression type. In this paper, we consider the latter class of observation-driven models: the integer-valued generalized autoregressive conditional heteroscedastic (INGARCH) models introduced by Heinen (2003) and Ferland et al. (2006) and defined as follows:

$$\begin{cases} X_t | \mathcal{F}_{t-1} : \text{Poisson}(\lambda_t), \\ \lambda_t = \alpha_0 + \sum_{i=1}^p \alpha_i X_{t-i} + \sum_{j=1}^q \beta_j \lambda_{t-j}, \end{cases} \quad (1.1)$$

where  $\mathcal{F}_{t-1}$  is the  $\sigma$ -field generated by  $\{X_{t-1}, X_{t-2}, \dots\}$ ,  $\alpha_0 > 0$ ,  $\alpha_i \geq 0$ ,  $\beta_j \geq 0$ , for  $i = 1, \dots, p$ ,  $j = 1, \dots, q$ ,  $p \geq 1$ ,  $q \geq 1$ . If  $q = 0$ , (1.1) is referred to as INARCH(p) (or INGARCH(p,0)) model. The term INGARCH was introduced by

Ferland et al. (2006) due to its similarity to the classical GARCH model proposed by Bollerslev (1986):

$$\begin{cases} X_t = \sigma_t \varepsilon_t, \\ \sigma_t^2 = \alpha_0 + \sum_{i=1}^p \alpha_i X_{t-i}^2 + \sum_{j=1}^q \beta_j \sigma_{t-j}^2, \end{cases}$$

where  $\sigma_t^2 = Var[X_t | \mathcal{F}_{t-1}]$  and  $\{\varepsilon_t\}$  is a sequence of white noise with mean 0 and variance 1. Further,  $\{X_s\}$  is independent of  $\{\varepsilon_t\}$  for every  $s < t$ . The model (1.1) is referred to as the Poisson INGARCH (PINGARCH) model where  $\lambda_t = E[X_t | \mathcal{F}_{t-1}]$ . Eventhough  $X_t$  conditioned on  $\mathcal{F}_{t-1}$  follows the equidispersed Poisson distribution with mean  $\lambda_t$ , it can model overdispersed counts (See Weiß and Schweer (2015)):

$$\mu_t = E[X_t] = E[\lambda_t], \quad Var[X_t] = \mu_t + Var[\lambda_t] > \mu_t.$$

Ferland et al. (2006) showed that if  $\sum_{i=1}^p \alpha_i + \sum_{j=1}^q \beta_j < 1$  is satisfied, the INGARCH process exists and is strictly stationary, with finite first and second - order moments. Then, the unconditional mean of  $X_t$  is given by

$$\mu = \frac{\alpha_0}{1 - \sum_{i=1}^p \alpha_i - \sum_{j=1}^q \beta_j}. \quad (1.2)$$

Further properties on variance and autocovariances as well as an in-depth review of the purely autoregressive case i.e PINARCH(p) (or PINGARCH(p,0) ) was conducted by Weiß (2009). Zhu (2011) proposed the negative binomial INGARCH (NB-INGARCH) model of the form:

$$\begin{cases} X_t | \mathcal{F}_{t-1} : NB(n, p_t), \\ \frac{1-p_t}{p_t} = \lambda_t = \alpha_0 + \sum_{i=1}^p \alpha_i X_{t-i} + \sum_{j=1}^q \beta_j \lambda_{t-j}, \end{cases} \quad (1.3)$$

where  $\mathcal{F}_{t-1}$ ,  $\alpha_0, \alpha_i, \beta_j$ , reprise the definition and conditions in (1.1) respectively. The parameter  $n$  is considered to be fixed, while  $p_t$  varies with time and  $p_t = 1/(1 + \lambda_t)$ . The conditional mean and variance respectively are

$$E[X_t | \mathcal{F}_{t-1}] = \frac{n(1-p_t)}{p_t} = n\lambda_t, \text{ and } Var[X_t | \mathcal{F}_{t-1}] = \frac{n(1-p_t)}{p_t^2} = n\lambda_t(1 + \lambda_t). \quad (1.4)$$

An alternate version of the negative binomial INGARCH was proposed by Xu et al. (2012) with the conditional distribution  $NB(n_t, p)$  with  $n_t = \lambda_t \frac{p}{1-p}$  and with the conditional mean  $\lambda_t$  satisfying right hand side of (1.3). In this article, we consider the model by Zhu (2011) for data analysis and comparison. Zhu (2012) defined the generalized Poisson (GP - INGARCH) model as

$$\begin{cases} X_t | \mathcal{F}_{t-1} : GP(\eta_t, \kappa), \\ \frac{\eta_t}{1-\kappa} = \lambda_t = \alpha_0 + \sum_{i=1}^p \alpha_i X_{t-i} + \sum_{j=1}^q \beta_j \lambda_{t-j}, \end{cases} \quad (1.5)$$

where  $p \geq 1, q \geq 1, \alpha_0 > 0, \max(-1, -\eta_t/4) < \kappa < 1, \alpha_i, \beta_j \geq 0, i = 1, \dots, p, j = 1, \dots, q$ , and  $\mathcal{F}_{t-1}$  is the past information. The probability mass function (pmf) of the generalized Poisson distribution ( $GP(\eta, \kappa)$ ) is defined as

$$Pr[X = x] = \begin{cases} \eta(\eta + \kappa x)^{x-1} e^{-(\eta + \kappa x)} / x!, & x = 0, 1, \dots, \\ 0, & \text{for } x > m \text{ if } \kappa < 0, \end{cases}$$

where  $\eta > 0$ ,  $\max(-1, -\eta/m) < \kappa < 1$ , and  $m(\geq 4)$  is the largest positive integer for which  $\eta + \kappa m > 0$  when  $\kappa < 0$ . It reduces to the usual Poisson with parameter  $\eta$  when  $\kappa = 0$ . Note that when  $\kappa < 0$ , the distribution is truncated because  $Pr[X = x] = 0$  for all  $x > m$ , making the sum  $\sum_{x=0}^m Pr[X = x]$  slightly less than 1. However, this truncation error is less than 0.5% when  $m \geq 4$ , so it is negligible in practical applications (Consul and Famoye, 2006). The respective conditional mean and conditional variance of  $\{X_t\}$  following (1.5) are

$$E[X_t | \mathcal{F}_{t-1}] = \frac{\eta_t}{1 - \kappa} = \lambda_t, \text{ and } Var[X_t | \mathcal{F}_{t-1}] = \frac{\eta_t}{(1 - \kappa)^3} = \frac{\lambda_t}{(1 - \kappa)^2}. \quad (1.6)$$

Detailed discussions and review of INGARCH models can be found in Weiß (2018) and Liu et al. (2023). In the following section, we introduce the novel geometric INGARCH (NoGe-INGARCH) model and discuss some of its properties. We then proceed to detail the estimation techniques in Section 3. Subsequently, Section 4 deals with simulation study. Section 5 emphasises the application through real data analysis. Section 6 concludes the study. Finally, Appendix A provides proofs of theorems and plots from the simulation study.

## 2. Novel geometric INGARCH model

The novel geometric distribution is defined by the pmf:

$$Pr[X = x] = \delta\phi + (1 - \delta)(1 - \phi)(1 - \theta)^{x-1}\theta, \quad x \in \mathbb{N}_0, \quad (2.1)$$

where  $0 < \phi < 1$  and  $0 < \theta \leq 1$ . The indicator function  $\delta$  assumes the value 1 when  $x = 0$  and 0 otherwise. The term “novel geometric” is carried forward from Andrews and Balakrishna (2023). We propose the NoGe-INGARCH model :

$$\begin{cases} X_t | \mathcal{F}_{t-1} : NoGe(\theta_t, \phi), \\ \frac{1-\phi}{\theta_t} = \lambda_t = \alpha_0 + \sum_{i=1}^p \alpha_i X_{t-i} + \sum_{j=1}^q \beta_j \lambda_{t-j}, \end{cases} \quad (2.2)$$

where  $\alpha_0 > 0$ ,  $\alpha_i \geq 0$ ,  $\beta_j \geq 0$ , for  $i = 1, \dots, p$ ,  $j = 1, \dots, q$ ,  $p \geq 1$ ,  $q \geq 1$ . The conditional mean and conditional variance of a NoGe-INGARCH( $p, q$ ) process  $\{X_t\}$  are:

$$E[X_t | \mathcal{F}_{t-1}] = \frac{1-\phi}{\theta_t} = \lambda_t, \text{ and } Var[X_t | \mathcal{F}_{t-1}] = \frac{1-\phi}{\theta_t} \left( \frac{1+\phi}{\theta_t} - 1 \right) = \lambda_t \left( \frac{1+\phi}{1-\phi} \lambda_t - 1 \right). \quad (2.3)$$

**Theorem 2.1.** *A necessary and sufficient condition for the NoGe-INGARCH( $p, q$ ) model (assuming  $p > q$ ) to be stationary in the mean is that the roots of the equation*

$$1 - \sum_{i=1}^q (\alpha_i + \beta_i) b^{-i} - \sum_{i=q+1}^p \alpha_i b^{-i} = 0, \quad (2.4)$$

*all lie inside the unit circle.*

Let  $\mu_t = E[X_t]$ . Then,

$$\begin{aligned}\mu_t &= E[X_t] = E[\lambda_t] \\ &= \alpha_0 + \sum_{i=1}^p \alpha_i E[X_{t-i}] + \sum_{i=q+1}^p \beta_i E[\lambda_{t-i}] = \alpha_0 + \sum_{i=1}^p \alpha_i \mu_{t-i} + \sum_{i=q+1}^p \beta_i \mu_{t-i}.\end{aligned}$$

The proof follows from the necessary and sufficient condition, discussed in [Goldberg \(1958\)](#), for a non-homogeneous difference equation to have a stable solution which is finite and independent of  $t$ , viz., the roots  $b_1, \dots, b_p$  of (2.4) all lie inside the unit circle.

*Remark 2.1.* Let the process  $\{X_t\}$  following the NoGe-INGARCH(p,q) model be first-order stationary. Then, we have the mean of the process as

$$\mu = E[X_t] = \frac{\alpha_0}{1 - \sum_{i=1}^p \alpha_i - \sum_{j=1}^q \beta_j}. \quad (2.5)$$

The following theorem states the second-order stationarity conditions for the NoGe-INGARCH model. To elucidate the core concept of the proof, a simplified NoGe-INARCH(p) model is considered.

**Theorem 2.2.** *Suppose that the process  $\{X_t\}$  following NoGe-INARCH(p) model is first-order stationary. Then, a necessary and sufficient condition for the process to be second-order stationary is that*

$$1 - L_1 b^{-1} - \dots - L_p b^{-p} = 0$$

has all roots lying inside the unit circle, where for  $r, s = 1, \dots, p-1$ ,  $L_r = \frac{2}{1-\phi} \left( \alpha_r^2 - \sum_{v=1}^{p-1} \sum_{|i-j|=v} \alpha_i \alpha_j m_{vr} \nu_{r0} \right)$ ,  $L_p = \frac{2\alpha_p^2}{1-\phi}$ ,  $\nu_{s0} = \alpha_s$ ,  $\nu_{ss} = \sum_{|i-s|=s} \alpha_i - 1$  and  $\nu_{sr} = \sum_{|i-s|=r} \alpha_i$ ,  $r \neq s$ . Also,  $M$  and  $M^{-1}$  are  $(p-1) \times (p-1)$  matrices such that  $M = (\nu_{ij})_{i,j=1}^{p-1}$  and  $M^{-1} = (m_{ij})_{i,j=1}^{p-1}$ .

The proof is given in [Appendix A.1](#). The next theorem states the structure of autocovariances of the NoGe-INGARCH model, given that it is second-order stationary.

**Theorem 2.3.** *Suppose that  $\{X_t\}$  following NoGe-INGARCH(p,q) process is second-order stationary. Let the autocovariances be defined as:*

$$\begin{aligned}\gamma_X(h) &= \text{Cov}[X_t, X_{t-h}], \text{ and} \\ \gamma_\lambda(h) &= \text{Cov}[\lambda_t, \lambda_{t-h}].\end{aligned}$$

Then, they satisfy the equations

$$\begin{aligned}\gamma_X(h) &= \sum_{i=1}^p \alpha_i \gamma_X(|h-i|) + \sum_{j=1}^{\min(h-1,q)} \beta_j \gamma_X(h-j) + \sum_{j=h}^q \beta_j \gamma_\lambda(j-h), \quad h \geq 1; \\ \gamma_\lambda(h) &= \sum_{i=1}^{\min(h,p)} \alpha_i \gamma_\lambda(|h-i|) + \sum_{i=h+1}^p \alpha_i \gamma_X(i-h) + \sum_{j=1}^q \beta_j \gamma_\lambda(|h-j|), \quad h \geq 0.\end{aligned}$$

The proof is detailed in [Appendix A.2](#). The following subsections show some of the properties of the NoGe-INGARCH(1,1), NoGe-INARCH(1) and NoGe-INARCH(2) models based on the theorems stated above.

### 2.1. NoGe-INGARCH (1,1)

Consider the NoGe-INGARCH (1,1) model:

$$\begin{cases} X_t | \mathcal{F}_{t-1} : NoGe(\theta_t, \phi), \\ \frac{1-\phi}{\theta_t} = \lambda_t = \alpha_0 + \alpha_1 X_{t-1} + \beta_1 \lambda_{t-1}, \end{cases}$$

where  $\alpha_0 > 0$ ,  $\alpha_1 \geq 0$  and  $\beta_1 \geq 0$ . By [Theorem 2.1](#), if the process  $\{X_t\}$  is stationary, we have

$$\mu = E[X_t] = \frac{\alpha_0}{1 - \alpha_1 - \beta_1}.$$

From [Theorem 2.3](#), we obtain

$$\gamma_X(h) = (\alpha_1 + \beta_1)^{h-1} \gamma_X(1), \quad h \geq 2, \quad \text{and} \quad \gamma_\lambda(h) = (\alpha_1 + \beta_1)^h \gamma_\lambda(0), \quad h \geq 1,$$

where  $\gamma_X(1) = \left(\frac{2\alpha_1}{1-\phi} + \beta_1\right) \gamma_\lambda(0) + \alpha_1 \mu \left(\frac{1+\phi}{1-\phi} \mu - 1\right)$ , and  $\gamma_\lambda(0) = \frac{\alpha_1^2 \mu \left((1+\phi)\mu - (1-\phi)\right)}{(1-\phi) \left(1 - (\zeta \alpha_1^2 + 2\alpha_1 \beta_1 + \beta_1^2)\right)}$ .

Then, for  $\zeta = \frac{2}{1-\phi}$ , the unconditional variance,  $Var[X_t] = \left(\frac{(1+\phi)}{(1-\phi)} \mu^2 - \mu\right) \frac{1 - (\zeta - 1) \alpha_1^2 - 2\alpha_1 \beta_1 - \beta_1^2}{1 - \zeta \alpha_1^2 - 2\alpha_1 \beta_1 - \beta_1^2}$ .

Further, the autocorrelations  $\rho_X(h) = (\alpha_1 + \beta_1)^h \frac{\alpha_1(1 - \alpha_1 \beta_1 - \beta_1^2)}{1 - (\zeta - 1) \alpha_1^2 - 2\alpha_1 \beta_1 - \beta_1^2}$ ,  $h \geq 1$ , and  $\rho_\lambda(h) = (\alpha_1 + \beta_1)^h$ ,  $h \geq 0$ .

### 2.2. NoGe-INARCH(1)

The simpler NoGe-INARCH (1) model is defined as:

$$\begin{cases} X_t | \mathcal{F}_{t-1} : NoGe(\theta_t, \phi), \\ \frac{1-\phi}{\theta_t} = \lambda_t = \alpha_0 + \alpha_1 X_{t-1}, \end{cases}$$

where  $\alpha_0 > 0$  and  $\alpha_1 \geq 0$ . Undoubtedly, it is a special case of NoGe-INGARCH(1,1) with mean, autocorrelations and variance respectively as:

$$E[X_t] = \frac{\alpha_0}{1 - \alpha_1}, \quad \rho_X(h) = \frac{\alpha_1^h}{1 - \frac{1+\phi}{1-\phi} \alpha_1^2}, \quad h \geq 1,$$

$$\text{and } Var[X_t] = \frac{\alpha_0}{1 - \alpha_1} \left( \frac{(1 + \phi)\alpha_0 - (1 - \phi)\alpha_1}{(1 - \phi)(1 - \alpha_1)} \right) \left( \frac{(1 - \phi) - (1 + \phi)\alpha_1^2}{(1 - \phi) - 2\alpha_1^2} \right).$$

### 2.3. NoGe-INARCH(2)

The NoGe-INARCH (2) model is specified by:

$$\begin{cases} X_t | \mathcal{F}_{t-1} : NoGe(\theta_t, \phi), \\ \frac{1-\phi}{\theta_t} = \lambda_t = \alpha_0 + \alpha_1 X_{t-1} + \alpha_2 X_{t-2}, \end{cases}$$

where  $\alpha_0 > 0$ ,  $\alpha_1 \geq 0$  and  $\alpha_2 \geq 0$ . In this case the mean and variance are:

$$E[X_t] = \frac{\alpha_0}{1 - \alpha_1 - \alpha_2}, \quad \text{and} \quad Var[X_t] = \left( \frac{(1 + \phi)}{(1 - \phi)} \mu^2 - \mu \right) \frac{1}{1 - (\alpha_1^2 + \alpha_2^2) - \frac{2\alpha_1\alpha_2}{1-\alpha_2}}.$$

The next section delves into the estimation techniques used for estimation of parameters of the model.

### 3. Estimation

In the present study, we have used two methods for estimation of parameters — conditional maximum likelihood and Bayesian estimation.

Let  $\boldsymbol{\alpha} = (\alpha_0, \alpha_1, \dots, \alpha_p)^T$ ,  $\boldsymbol{\beta} = (\beta_1, \dots, \beta_q)^T$ ,  $\boldsymbol{\theta} = (\boldsymbol{\alpha}^T, \boldsymbol{\beta}^T)^T = (\theta_0, \theta_1, \dots, \theta_{p+q})^T$ ,  $\boldsymbol{\Theta} = (\phi, \boldsymbol{\theta})^T = (\Theta_1, \Theta_2, \dots, \Theta_{p+q+2})^T$ . To estimate  $\boldsymbol{\Theta}$ , we will first define the conditional log - likelihood function

$$L(\boldsymbol{\Theta} | \mathcal{F}_{t-1}) = \prod_{t=1}^n Pr[X_t = x_t | \mathcal{F}_{t-1}] = \prod_{t=1}^n \phi^{\delta_t} \left[ (1 - \phi)^2 \left( 1 - \frac{1 - \phi}{\lambda_t} \right)^{x_t - 1} \frac{1}{\lambda_t} \right]^{(1 - \delta_t)}, \quad (3.1)$$

where  $\lambda_t$  is updated according to definition in (2.2),  $\delta_t$  is the indicator function assuming 1 when  $x_t = 0$  and 0 otherwise, and  $0 < \phi < 1$ . This implies that the conditional log - likelihood is of the form

$$\begin{aligned} l(\boldsymbol{\Theta} | \mathcal{F}_{t-1}) &= \log L(\boldsymbol{\Theta} | \mathcal{F}_{t-1}) \\ &= \sum_{t=1}^n \left\{ \delta_t \log \phi + (1 - \delta_t) \left[ 2 \log(1 - \phi) + (x_t - 1) \log \left( 1 - \frac{1 - \phi}{\lambda_t} \right) - \log(\lambda_t) \right] \right\}. \end{aligned} \quad (3.2)$$

The conditional maximum likelihood estimates (CMLEs) of the parameter vector  $\boldsymbol{\Theta}$  can be found by maximizing  $l(\boldsymbol{\Theta} | \mathcal{F}_{t-1})$  specified in (3.2). However, it is easy to see that the estimates have no closed form and numerical optimization methods have to be used. In the following subsection, we develop an algorithm for numerical optimization of log-likelihood function using Bayesian methods.

#### 3.1. The Hamiltonian Monte Carlo (HMC) algorithm

Let  $\mathcal{P}_0(\boldsymbol{\Theta})$  denote the prior density of  $\boldsymbol{\Theta}$ . By Bayes' rule, the posterior density of  $\boldsymbol{\Theta}$  given the data is proportional to the product of the likelihood function and the prior, i.e.,

$$\mathcal{P}(\boldsymbol{\Theta} | \mathcal{F}_{t-1}) \propto L(\boldsymbol{\Theta} | \mathcal{F}_{t-1}) \mathcal{P}_0(\boldsymbol{\Theta}). \quad (3.3)$$

In general, we assume multivariate normal non-informative priors with large variances for the parameters (Andrade et al., 2023). However, one must bear in mind that for the model proposed in (2.2), all parameters are assumed non-negative or strictly positive (in the case of  $\alpha_0$ ) real-valued. In addition, constraints imposed by the stationarity conditions on the parameters and that the parameter  $\phi$  is always bounded between 0 and 1 should also be speculated. So, we transform the constrained parameters to the real space by suitable functions such as logit, square root etc. depending on the bounds imposed by the conditions. Then, we proceed to assign normal priors to the transformed unconstrained parameters. In the present article, we have considered logit transformations to the constrained parameters with the exception of the intercept  $\alpha_0$  for which a log-normal prior is assumed. The task that remains is to draw samples from the posterior distribution.

Statistical models with complex posterior distributions often rely on Markov chain Monte Carlo (MCMC) methods, detailed by Gelfand and Smith (1990), to sample from these distributions. The Metropolis-Hastings(MH) algorithm, discussed by Tierney (1994) as a versatile method for creating Markov chains from

the target distribution  $\mathcal{P}(\Theta)$ , is commonly employed. The algorithm employs a “jumping distribution”  $\mathfrak{p}(\Theta^*|\Theta)$  to enable transitions from a current parameter state  $\Theta$  to a proposed state  $\Theta^*$  within the parameter space. These proposed transitions are accepted with a probability  $\min\left(1, \frac{\mathfrak{p}(\Theta|\Theta^*)}{\mathfrak{p}(\Theta^*|\Theta)}\right)$ . A likely choice for  $\mathfrak{p}(\cdot)$  is a normal distribution rendering the sequence of samples into a Gaussian random walk (Chib and Greenberg, 1995).

The random walk Metropolis is easy to implement and has an intuitive appeal. It tends to propose points in regions with large volumes, often pushing proposals towards the tails of the target distribution. The Metropolis correction step then rejects proposals that fall into low-density areas, favoring those within high-probability regions, thereby concentrating towards the typical set of the target distribution. However, as the dimensionality of the target distribution increases, the volume outside the typical set becomes dominant, causing most proposals to land in low-density tail regions, resulting in very low acceptance probabilities and frequent rejections. Reducing the step size,  $\epsilon$ , (specified based on the required level of accuracy) of proposals can increase acceptance by staying within the typical set, but this slows down the movement of the Markov chain significantly leading to highly biased MCMC estimators. (Betancourt, 2017)

The HMC algorithm, initially known as Hybrid Monte Carlo (Duane et al., 1987), extends the MH algorithm by generating more accurate proposal values through the use of Hamiltonian dynamics. It introduces a momentum variable  $\nu_j$  for each component  $\Theta_j$  in the target space. These variables  $\Theta_j$  and  $\nu_j$  are simultaneously updated using a modified MH algorithm, where the jumping distribution for  $\Theta$  is heavily influenced by  $\nu$ . Essentially, the momentum  $\nu$  indicates the expected distance and direction of jump in  $\Theta$ , promoting consecutive jumps in a consistent direction and facilitating rapid movement across the  $\Theta$  space when feasible. This is implemented using the leapfrog algorithm. Thus, it succeeds in suppressing the random walk behaviour. The MH accept/reject rule halts movement upon entering low-probability regions, prompting momentum adjustments until transition can resume (Gelman et al., 2013).

In short, in the above sampling strategy, proposal distributions are directed towards the mode(s) of the posterior distribution rather than being symmetrical around the current position. These proposals utilize trajectories derived from the gradient of the posterior, and then employs the MH method to accept or reject these choices (Neal, 2011). Thus, compared to MH algorithms, HMC offers a more efficient approach to Monte Carlo sampling. (Kruschke, 2014)

The Hamiltonian function (See Andrade et al. (2023)) can be written as :

$$\mathcal{H}(\Theta, \nu) = \mathcal{U}(\Theta) + \mathcal{K}(\nu), \quad (3.4)$$

where  $\mathcal{H}(\cdot)$  denotes the total energy of the system,  $\mathcal{U}(\cdot)$  represents the potential energy and  $\mathcal{K}$  the kinetic energy respectively. The changes in  $\Theta$  and  $\nu$  over iterations  $\tau$  are governed by Hamilton’s equations, which are derived from the

partial derivatives of the Hamiltonian:

$$\begin{aligned}\frac{d\Theta}{d\tau} &= \frac{\partial\mathcal{H}(\Theta, \boldsymbol{\nu})}{\partial\boldsymbol{\nu}}, \\ \frac{d\boldsymbol{\nu}}{d\tau} &= -\frac{\partial\mathcal{H}(\Theta, \boldsymbol{\nu})}{\partial\Theta}.\end{aligned}\tag{3.5}$$

During any time interval  $\Delta\tau$ , these equations describe a change from the state at time  $\tau$  to that at  $\tau + \Delta\tau$ . In Bayesian analysis, the parameter  $\Theta$  is analogous to positions. The posterior distribution (3.3) can be represented as a canonical distribution by employing a potential energy function as:

$$\mathcal{U}(\Theta) = -\log(\mathcal{P}(\Theta | \mathcal{F}_{t-1})) = -\log(L(\Theta | \mathcal{F}_{t-1})\mathcal{P}_0(\Theta)) + \mathcal{C},$$

where  $\mathcal{C}$  represents a normalizing constant, and the kinetic energy is given by

$$\mathcal{K}(\boldsymbol{\nu}) = \frac{\boldsymbol{\nu}^T \Sigma^{-1} \boldsymbol{\nu}}{2},\tag{3.6}$$

where the generalized moment  $\boldsymbol{\nu}$  will be expressed as a normal random variable  $\mathcal{Z} \sim N(\mathbf{0}, \Sigma)$  of the same dimension as  $\Theta$ , the parameter vector of interest. This yields equations (3.4) and (3.5) as

$$\mathcal{H}(\Theta, \boldsymbol{\nu}) = -\log(\mathcal{P}(\Theta | \mathcal{F}_{t-1})) + \frac{\boldsymbol{\nu}^T \Sigma^{-1} \boldsymbol{\nu}}{2},$$

and

$$\begin{aligned}\frac{d\Theta}{d\tau} &= \frac{\partial\mathcal{H}(\Theta, \boldsymbol{\nu})}{\partial\boldsymbol{\nu}} = \Sigma^{-1}\boldsymbol{\nu}, \\ \frac{d\boldsymbol{\nu}}{d\tau} &= -\frac{\partial\mathcal{H}(\Theta, \boldsymbol{\nu})}{\partial\Theta} = \nabla_{\Theta}\log(\mathcal{P}(\Theta | \mathcal{F}_{t-1})),\end{aligned}\tag{3.7}$$

where  $\nabla_{\Theta}\log(\mathcal{P}(\Theta | \mathcal{F}_{t-1})) = (l_i + \partial\log\mathcal{P}_0(\Theta)/\partial\Theta_i)$  is the log posterior gradient with  $l_i = \partial l(\Theta | \mathcal{F}_{t-1})/\partial\Theta_i$  for  $i = 1, 2, \dots, p + q + 2$ . In most cases, solving (3.7) requires numerical methods, and one such method mentioned earlier is the leapfrog integrator. For a given number of steps  $\mathcal{L}$ , and step size  $\epsilon$ , the leapfrog integrator simulates the exact trajectory as (See [Betancourt \(2017\)](#)):

```

 $\theta_0 \leftarrow \theta, \nu_0 \leftarrow \nu$ 
for  $0 \leq n < \lfloor \mathcal{L}/\epsilon \rfloor$  do
   $\nu_{n+\frac{1}{2}} \leftarrow \nu_n - \frac{\epsilon}{2} \frac{\partial\mathcal{P}(\theta_n)}{\partial\theta}$ 
   $\theta_{n+1} \leftarrow \theta_n + \epsilon\nu_{n+\frac{1}{2}}$ 
   $\nu_{n+1} \leftarrow \nu_{n+\frac{1}{2}} - \frac{\epsilon}{2} \frac{\partial\mathcal{P}(\theta_{n+1})}{\partial\theta}$ 
end for

```

Here,  $\mathcal{L}$  and  $\epsilon$  are parameters of the algorithm, which need to be tuned to get good performance. The no - U - Turn sampler (NUTS) was introduced to reduce Hamiltonian Monte Carlo's reliance on two specific parameters ([Hoffman and Gelman, 2014](#)). Instead of employing a fixed step size, this sampler initially explores the sampling space and adjusts the step size to achieve a target acceptance rate (typically set at 0.8), which has been demonstrated to be optimal ([Betancourt et al.,](#)



2014). Subsequently, the no-U-turn sampler utilizes a recursive tree-building algorithm that progressively increases the trajectory length until a U-turn is detected. The occurrence of a U - turn signals inefficient exploration, prompting the algorithm to adapt the trajectory length within an optimal range. The probabilistic programming language, Stan, uses NUTS technique to conduct Bayesian optimization and leverages automatic differentiation techniques to compute gradients of the posterior distribution with respect to model parameters. This feature enables efficient exploration of the parameter space and helps in obtaining more accurate and reliable estimates of posterior quantities.(Gelman et al., 2015).

### 3.1.1. Stan

The Stan reference manual (Stan Development Team, 2024) mentions that Stan is named after Stanislaw Ulam (1909-1984), a seminal figure in the development of Monte Carlo techniques of Monte Carlo methods. While it's also been interpreted as the acronym "Sampling Through Adaptive Neighborhoods" (Gelman et al., 2013).

To utilize Stan, a user creates a Stan script that directly evaluates the log-posterior density. This script is then compiled and executed alongside the relevant dataset. The output consists of posterior simulations for the model parameters, or alternatively, a single point estimate if Stan is configured for optimization. Stan is compatible with command line usage as well as integration with R, Python, MATLAB, or Julia, facilitating storage, printing, or visualization of results. In this article, the rstan package (Stan Development Team, 2016) within the R software is used to call Stan functions and generate simulated data responses. The following section explains the Monte Carlo simulation study conducted for the model using the two estimation techniques.

## 4. Simulation Study

A simulation study was conducted to evaluate the finite sample performance of the estimators. We consider the following models:

(I) INARCH(1) model:

- NoGe-INARCH model with  $(\alpha_0, \alpha_1, \phi)^T = (2, 0.6, 0.3)^T$

(II) INARCH(2) model:

- NoGe-INARCH model with  $(\alpha_0, \alpha_1, \alpha_2, \phi)^T = (3, 0.45, 0.4, 0.6)^T$

(III) INGARCH(1,1) model:

- NoGe-INGARCH model with  $(\alpha_0, \alpha_1, \beta_1, \phi)^T = (1, 0.7, 0.2, 0.55)^T$

The evaluation criteria, in the case of CMLE, are the mean absolute bias (Abs. Bias) and the mean squared error (MSE) defined as:

$$Abs.Bias(\hat{\Theta}) = \frac{1}{N} \sum_{k=1}^N |\hat{\Theta}_i^{(k)} - \Theta_i^0|,$$

and

$$MSE(\hat{\Theta}) = \frac{1}{N} \sum_{k=1}^N (\hat{\Theta}_i^{(k)} - \Theta_i^0)^2,$$

respectively, where  $N$  is the number of replications,  $\hat{\Theta}_i^{(k)}$  is the CMLE corresponding to the  $k^{th}$  Monte Carlo replicate, for  $i = 1, \dots, p + q + 2$  and  $\Theta_i^0$  is the true value of the  $i^{th}$  parameter. For the present study, we have considered  $N = 1000$ . Following [Andrade et al. \(2023\)](#), the corresponding metrics for evaluating the Bayesian estimates are the square - root of the mean - squared error (RMSE) and mean absolute bias. In the context of Bayesian analysis,  $\hat{\Theta}_i^{(k)}$  are the respective posterior mean of the estimate of  $\Theta_i^0$  under squared error loss. To obtain Monte Carlo estimates from the posterior means, we generated 25,000 MCMC iterations of the model parameter vector from the complete posterior distribution using the Hamiltonian Monte Carlo (HMC) algorithm. We discarded the initial 50% of the MCMC iterations as burn-in, resulting in a chain comprising 12,500 posterior samples each of sizes 50, 100 and 500 for each replication. The posterior samples were utilized to compute the Monte Carlo estimates of the posterior mean for each model parameter. The results are exhibited in [Tables 1 to 3](#) respectively for the various scenarios listed above. Since optimisation of conditional maximum likelihood estimates consumed a lot of time (approximately 12 hrs per simulation for samples sized 50) in R, the simulation exercise was done in MATLAB, whereas the Bayesian analysis was carried out by the R interface of Stan, viz., rstan.

From [Tables 1, 2 and 3](#), it is clear that the absolute biases, MSE and RMSE of the estimates decrease with increase in sample size. In the case of Bayesian estimation by HMC algorithm, the convergence of Markov chains to the stationary distributions of interest are checked using histograms of the posterior distributions, traceplots and autocorrelation of parameters for the three cases and are given in [Appendix A.3](#). Autocorrelation function (ACF) plots visualize the autocorrelation of MCMC chains. High autocorrelation indicates poor mixing, while low autocorrelation suggests better convergence. The ACF plots in [Figures 9, 12 and 15](#) show that the chains behave well, as autocorrelation quickly drops to zero with increasing lag.

Table 1: Simulation results for (I) INARCH(1) model.

Sample size	Parameter	CMLE			Bayesian Estimates		
		Avg. Est.	MSE	Abs. Bias	Avg. Est.	RMSE	Abs. Bias
50	$\alpha_0 = 2$	2.0400	0.1855	0.3289	2.0054	0.0095	0.0119
	$\alpha_1 = 0.6$	0.5550	0.0763	0.2252	0.5184	0.0816	0.0820
	$\phi = 0.3$	0.2987	0.0041	0.0501	0.3098	0.0475	0.0614
100	$\alpha_0 = 2$	2.0255	0.0787	0.2219	2.0046	0.0090	0.0110
	$\alpha_1 = 0.6$	0.5785	0.0390	0.1582	0.5192	0.0808	0.0812
	$\phi = 0.3$	0.3008	0.0021	0.0361	0.2913	0.0334	0.0414
500	$\alpha_0 = 2$	2.0073	0.0152	0.0972	2.0026	0.0071	0.0093
	$\alpha_1 = 0.6$	0.5958	0.0071	0.0680	0.5194	0.0806	0.0811
	$\phi = 0.3$	0.3006	0.0004	0.0162	0.2956	0.0162	0.0209

Table 2: Simulation results for (II) INARCH(2) model.

Sample size	Parameter	CMLE			Bayesian Estimates		
		Avg. Est.	MSE	Abs. Bias	Avg. Est.	RMSE	Abs. Bias
50	$\alpha_0 = 3$	3.0871	0.6046	0.5967	2.9877	0.0151	0.0183
	$\alpha_1 = 0.45$	0.3640	0.1056	0.2793	0.4563	0.0083	0.0105
	$\alpha_2 = 0.40$	0.3268	0.0988	0.2711	0.3869	0.0131	0.0143
	$\phi = 0.6$	0.5992	0.0051	0.0565	0.5976	0.0523	0.0657
100	$\alpha_0 = 3$	3.0959	0.2957	0.4305	2.9888	0.0148	0.0180
	$\alpha_1 = 0.45$	0.3837	0.0718	0.2229	0.4559	0.0077	0.0097
	$\alpha_2 = 0.40$	0.3429	0.0666	0.2155	0.3873	0.0127	0.0140
	$\phi = 0.6$	0.6002	0.0024	0.0399	0.5922	0.0381	0.0484
500	$\alpha_0 = 3$	3.0159	0.0586	0.1926	2.9897	0.0135	0.0168
	$\alpha_1 = 0.45$	0.4477	0.0143	0.0959	0.4554	0.0069	0.0087
	$\alpha_2 = 0.40$	0.3945	0.0213	0.1162	0.3881	0.0120	0.0130
	$\phi = 0.6$	0.6003	0.0005	0.0178	0.5976	0.0189	0.0243

Table 3: Simulation results for (III) INGARCH(1,1) model.

Sample size	Parameter	CMLE			Bayesian Estimates		
		Avg. Est.	MSE	Abs. Bias	Avg. Est.	RMSE	Abs. Bias
50	$\alpha_0 = 1$	0.9609	0.1817	0.3513	0.9945	0.0055	0.0061
	$\alpha_1 = 0.7$	0.5984	0.0910	0.2365	0.6342	0.1658	0.1659
	$\beta_1 = 0.2$	0.2226	0.0621	0.1961	0.1585	0.0415	0.0416
	$\phi = 0.55$	0.5471	0.0049	0.0563	0.5628	0.0540	0.0660
100	$\alpha_0 = 1$	1.0053	0.1008	0.2591	0.9946	0.0054	0.0058
	$\alpha_1 = 0.7$	0.6350	0.0531	0.1818	0.6535	0.1648	0.1649
	$\beta_1 = 0.2$	0.2056	0.0370	0.1533	0.1683	0.0317	0.0217
	$\phi = 0.55$	0.5496	0.0026	0.0411	0.5424	0.0419	0.0511
500	$\alpha_0 = 1$	1.0229	0.0508	0.1732	0.9948	0.0053	0.0057
	$\alpha_1 = 0.7$	0.6491	0.0057	0.0608	0.6839	0.1616	0.1562
	$\beta_1 = 0.2$	0.2022	0.0095	0.0756	0.1883	0.0217	0.0108
	$\phi = 0.55$	0.5501	0.0004	0.0163	0.5498	0.0180	0.0229

Trace plots display parameter values across iterations, showing how the MCMC samples evolve. The trace plots in Figures 8, 11 and 14 appear random and well-mixed, with values fluctuating around a central point, indicating no anomalies. Posterior histograms illustrate parameter uncertainty in Bayesian models. The histograms in Figures 7, 10 and 13 are stable, showing convergence, with peaks around the most probable values and mostly narrow widths, indicating low uncertainty. In what follows, we elucidate the application of the proposed model and estimation methods to real datasets.

## 5. Data Analysis

For the real data application, we consider two data sets viz., weekly data on Hepatitis - B cases and a data on the number of transactions of a stock . We fit four models to the data sets — NoGe-INGARCH, GP-INGARCH, NB-INGARCH and PINGARCH each with  $p = 1$  and  $q = 1$ . The model adequacy criteria are Akaike information criterion (AIC) (Akaike (1974)) and expected Bayesian information criterion (EBIC) (Carlin and Louis (2008)). EBIC is estimated from the HMC output as

$$\widehat{EBIC} = \frac{1}{M} \sum_{m=1}^M -2l(\Theta | \mathcal{F}_{t-1}) + \mathbf{p} \log(n),$$

where  $l(\Theta | \mathcal{F}_{t-1})$  is the conditional log-likelihood function in evaluated using the generated chain from HMC procedure  $\{\Theta^{(m)}, m = 1, \dots, M\}$ ,  $\mathbf{p}$  is the number of parameters in the model and  $n$  is the total number of observations.

### 5.1. Analysis of Hepatitis - B cases

Hepadnaviruses (Hepatitis- B) viruses, can lead to both temporary and long-term liver infections. Temporary infections can result in severe illness, with about 0.5% leading to fatal, rapid-onset hepatitis. Chronic infections also pose significant risks, as nearly 25% result in incurable liver cancer.(See Seeger and Mason (2000)). For the present study, the weekly number of hepatitis - B cases reported in the states of Bremen, Hamburg and Saxony-Anhalt from January 2017 to February 2019 is considered.

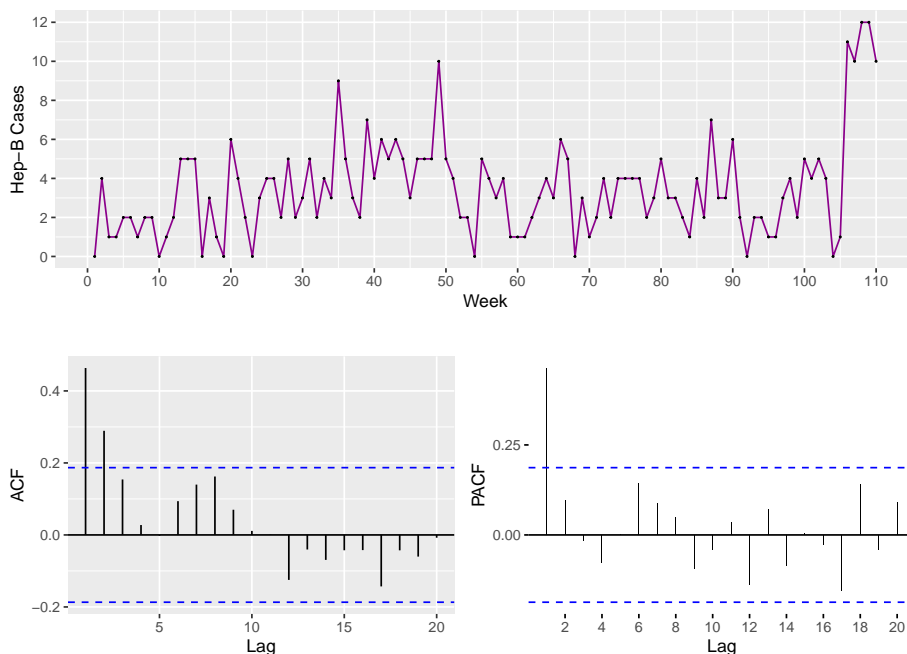


Figure 1: Time series, ACF and PACF plots of Hepatitis-B data.

The data, consisting of 110 observations, is available at <https://survstat.rki.de>. Figure 1 depicts the timeseries, ACF and partial autocorrelation function (PACF)

plots of the data. Table 4 gives the parameter estimates with their corresponding standard errors and posterior standard deviations (for Bayesian estimates) in square brackets respectively, along with AIC and EBIC criteria. From Table 4, we can observe that eventhough GP-INGARCH has the least AIC, it has higher EBIC value as compared to the other models. NB-INGARCH performs well in terms of EBIC criterion. Notably, NoGe-INGARCH(1,1) provides nearer to minimum values for both criteria.

Table 4: CMLEs, Bayesian estimates, AIC and EBIC of various models fitted to Hepatitis data.

Model	Conditional Maximum Likelihood Estimates				Bayesian Estimates				AIC	EBIC
	Parameter				Parameter					
	1	2	3	4	1	2	3	4		
NoGe - INGARCH(1,1) ( $\alpha_0, \alpha_1, \beta_1, \phi$ )	1.5811 [0.8455]	0.3806 [0.1011]	0.1787 [0.2914]	0.7239 [0.0995]	1.9134 [0.0417]	0.3089 [0.0082]	0.1521 [0.0208]	0.0734 [0.0009]	469.56	504.55
GP-INGARCH(1,1) ( $\alpha_0, \alpha_1, \beta_1, \kappa$ )	1.5750 [0.2169]	0.3827 [0.0213]	0.1796 [0.2540]	0.1522 [0.0120]	1.8663 [0.0352]	0.4046 [0.0186]	0.0762 [0.0227]	0.1607 [0.0052]	469.44	508.76
NB-INGARCH(1,1) ( $\alpha_0, \alpha_1, \beta_1, n$ )	1.6654 [1.0785]	0.3471 [0.1096]	0.1842 [0.3799]	9.8134 [5.2994]	1.9095 [0.0718]	0.3824 [0.0037]	0.0792 [0.0198]	9.9657 [0.1832]	470.86	503.03
PINGARCH(1,1) ( $\alpha_0, \alpha_1, \beta_1$ )	1.5251 [0.8137]	0.3636 [0.0914]	0.2122 [0.2890]		1.8107 [0.0346]	0.4055 [0.0038]	0.0878 [0.0010]		474.36	507.38

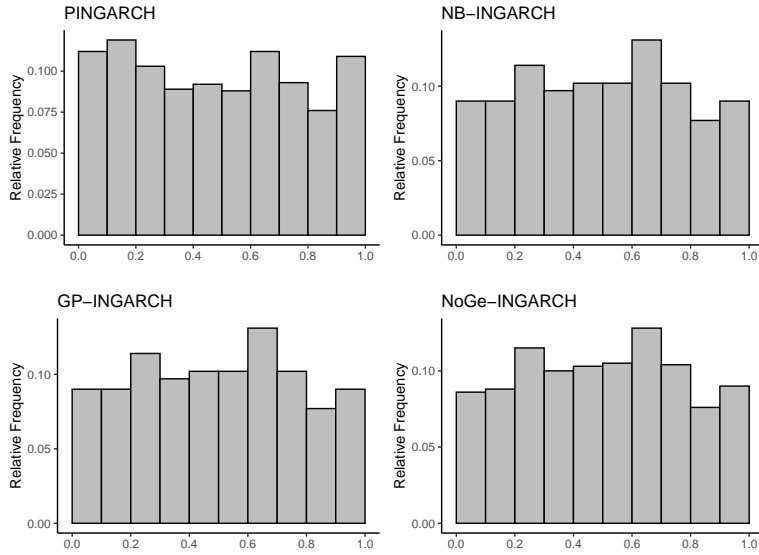


Figure 2: PIT histograms of models fitted to Hepatitis-B data.

Figures 2 and 3 display the PIT histograms and ACF plots of residuals of the models respectively. The PIT histograms conform to uniform distribution behaviour for most cases, and the acf plots are all shown to be stationary with no significant lags greater than zero.

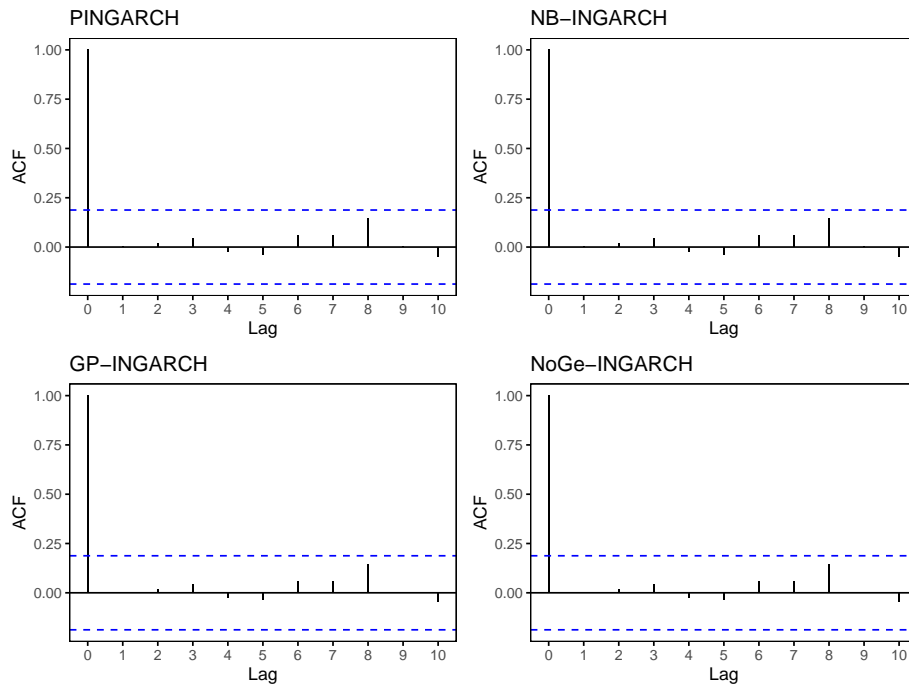


Figure 3: ACF plots of residuals of models fitted to Hepatitis-B data.

### 5.2. Analysis of Transactions data

The number of transactions of the Ericsson - B stock per minute between 9:35 and 17:14 on 2 July 2002, encompassing 460 observations sourced from [Weiß \(2018\)](#). [Figure 4](#) shows the timeseries, ACF and PACF plots corresponding to the count time series.

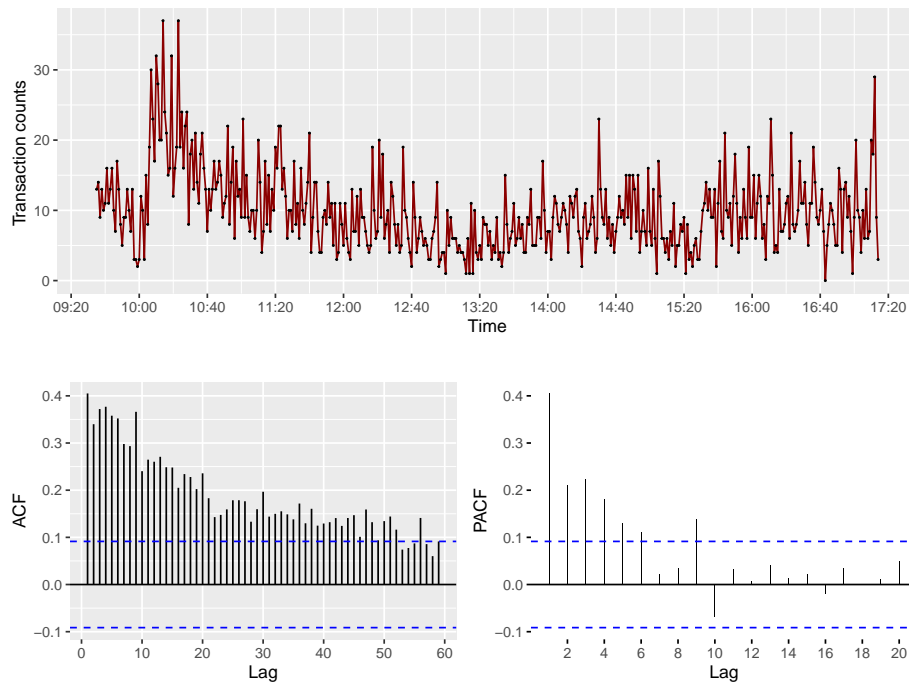


Figure 4: Time series, ACF and PACF plots of Transactions data.

The data was originally published by Brännäs and Quoreshi (2010) and provides the data for working days between 2 and 22 July 2002. Weiß (2018) concluded that the GP-INGARCH(1,1) model fits the data well, based on the AIC. Table 5 enlists the parameter estimates with their corresponding standard errors and posterior standard deviations in square brackets. The minimum AIC and EBIC corresponds to NoGe-INGARCH(1,1) and differs from GP-INGARCH(1,1) only by a margin. From Figure 5, it can be seen that the PIT histograms of NoGe-INGARCH(1,1), GP-INGARCH(1,1) and NB-INGARCH(1,1) conform to the uniform pattern. A conclusion similar to the previous analysis that the residuals are uncorrelated can be arrived at by inspection of Figure 6.

Table 5: CMLEs, Bayesian estimates, AIC and EBIC of various models fitted to Transactions data.

Model	Conditional Maximum Likelihood Estimates				Bayesian Estimates				AIC	EBIC
	Parameter				Parameter					
	1	2	3	4	1	2	3	4		
NoGe - INGARCH(1,1) $(\alpha_0, \alpha_1, \beta_1, \phi)$	0.3008 [0.1522]	0.1390 [0.0161]	0.8420 [0.0226]	0.1008 [0.0141]	0.2780 [0.0017]	0.1051 [0.0007]	0.8663 [0.0007]	0.0022 [0.0000]	2657.35	2681.78
GP-INGARCH(1,1) $(\alpha_0, \alpha_1, \beta_1, \kappa)$	0.2930 [0.1436]	0.1324 [0.0265]	0.8376 [0.0343]	0.3381 [0.0234]	0.2535 [0.0043]	0.1071 [0.0006]	0.8672 [0.0009]	0.3425 [0.0011]	2662.15	2688.38
NB-INGARCH(1,1) $(\alpha_0, \alpha_1, \beta_1, n)$	0.2697 [0.1424]	0.1272 [0.0257]	0.8453 [0.0336]	7.8606 [0.9593]	0.2376 [0.0025]	0.1078 [0.0007]	0.8678 [0.0007]	7.8136 [0.0346]	2665.82	2691.71
PINGARCH(1,1) $(\alpha_0, \alpha_1, \beta_1)$	0.2922 [0.1001]	0.1388 [0.0178]	0.8318 [0.0233]		0.2463 [0.0032]	0.1199 [0.0022]	0.8551 [0.0023]		2866.15	2887.11

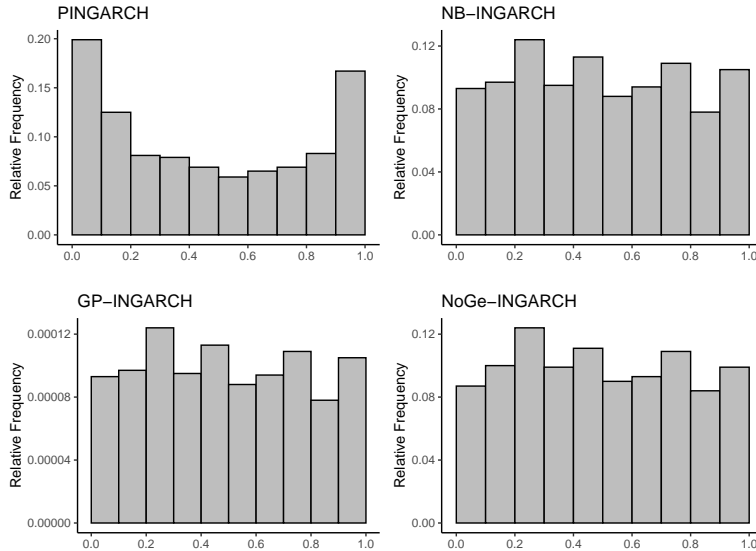


Figure 5: PIT histograms following analysis of Transactions data.

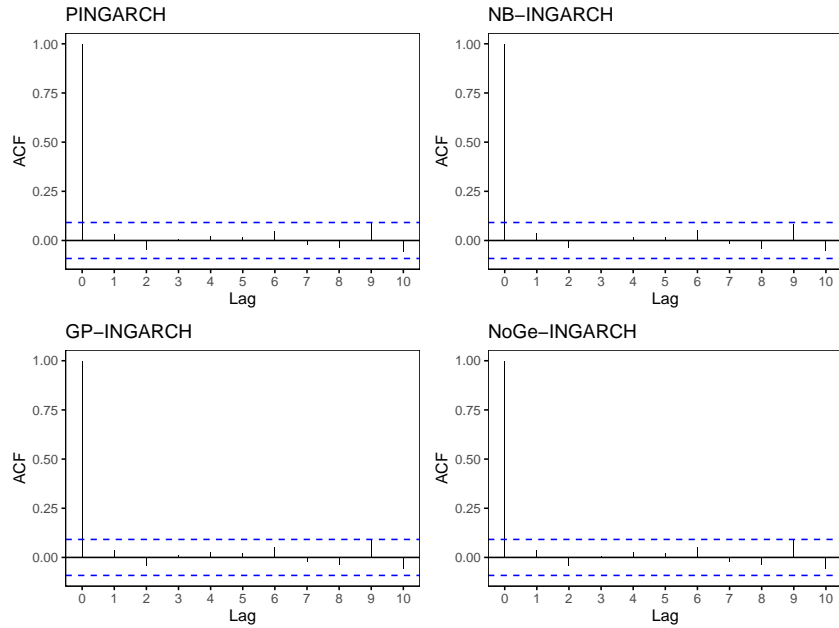


Figure 6: ACF plots of residuals of models following analysis of Transactions data.

## 6. Conclusion

In this paper, we introduced a novel geometric INGARCH (NoGe-INGARCH) process and discussed some statistical properties. The methods of estimation by conditional maximum likelihood and Bayesian approach via HMC algorithm in the context of INGARCH models were detailed. A simulation study was conducted to compare the estimation procedures in the case of NoGe-INGARCH model. Real data analysis was performed on two data sets to show the application of the NoGe-INGARCH model and compare it with other existing models in terms of goodness of fit.

## Declaration of interest

No potential conflict of interest was reported by the authors.

## Acknowledgement

The first author wishes to thank Cochin University of Science and Technology, India, for the financial support.

## References

- Akaike, H. (1974). A new look at the statistical model identification. *IEEE Transactions on Automatic Control*, 19(6):716–723.
- Andrade, M. G., Conceição, K. S., and Ravishanker, N. (2023). Zero-modified count time series modeling with an application to influenza cases. *AStA Advances in Statistical Analysis*, pages 1–27.



- Andrews, D. K. and Balakrishna, N. (2023). A novel geometric AR(1) model and its estimation. *Journal of Statistical Computation and Simulation*, 93(16):2906–2935.
- Betancourt, M. (2017). A conceptual introduction to Hamiltonian Monte Carlo. *arXiv preprint arXiv:1701.02434*.
- Betancourt, M. J., Byrne, S., and Girolami, M. (2014). Optimizing the integrator step size for Hamiltonian Monte Carlo. *arXiv preprint arXiv:1411.6669*.
- Bollerslev, T. (1986). Generalized autoregressive conditional heteroskedasticity. *Journal of Econometrics*, 31(3):307–327.
- Brännäs, K. and Quoreshi, A. S. (2010). Integer-valued moving average modelling of the number of transactions in stocks. *Applied Financial Economics*, 20(18):1429–1440.
- Carlin, B. P. and Louis, T. A. (2008). *Bayes and Empirical Bayes methods for Data Analysis*. CRC press.
- Chib, S. and Greenberg, E. (1995). Understanding the metropolis-hastings algorithm. *The American Statistician*, 49(4):327–335.
- Consul, P. and Famoye, F. (2006). *Lagrangian Probability Distributions*. Birkhäuser, Boston, MA.
- Duane, S., Kennedy, A. D., Pendleton, B. J., and Roweth, D. (1987). Hybrid Monte Carlo. *Physics Letters B*, 195(2):216–222.
- Ferland, R., Latour, A., and Oraichi, D. (2006). Integer-valued GARCH process. *Journal of Time Series Analysis*, 27(6):923–942.
- Fong, P. W., Li, W. K., Yau, C., and Wong, C. S. (2007). On a mixture vector autoregressive model. *Canadian Journal of Statistics*, 35(1):135–150.
- Gelfand, A. E. and Smith, A. F. (1990). Sampling-based approaches to calculating marginal densities. *Journal of the American Statistical Association*, 85(410):398–409.
- Gelman, A., Carlin, J. B., Stern, H. S., Dunson, D. B., Vehtari, A., and Rubin, D. B. (2013). *Bayesian Data Analysis*. CRC Press, Boca Raton, FL, 3rd edition.
- Gelman, A., Lee, D., and Guo, J. (2015). Stan: A probabilistic programming language for bayesian inference and optimization. *Journal of Educational and Behavioral Statistics*, 40:530–543.
- Goldberg, S. (1958). *Introduction to Difference Equations*. John Wiley & Sons, Inc., New York.

- Heinen, A. (2003). Modelling Time Series Count Data: An Autoregressive Conditional Poisson Model. In *CORE Discussion Papers*, 2003/62, University of Louvain, Belgium.
- Hoffman, M. D. and Gelman, A. (2014). The no-U-turn sampler: Adaptively setting path lengths in Hamiltonian Monte Carlo. *Journal of Machine Learning Research*, 15:1593–1623.
- Kruschke, J. (2014). Doing Bayesian data analysis: A tutorial with R, JAGS, and Stan.
- Liu, M., Zhu, F., Li, J., and Sun, C. (2023). A systematic review of INGARCH models for integer-valued time series. *Entropy*, 25(6):922.
- Neal, R. M. (2011). *Handbook of Markov Chain Monte Carlo*, chapter 5, page 113–162. CRC Press/Taylor & Francis, Boca Raton, FL.
- Seeger, C. and Mason, W. S. (2000). Hepatitis b virus biology. *Microbiology and Molecular Biology Reviews*, 64(1):51–68.
- Stan Development Team (2016). rstan: R interface to Stan (R package version 2.0.3). Retrieved from <http://mc-stan.org>.
- Stan Development Team (2024). Stan Reference Manual (Version 2.34). Retrieved from <https://mc-stan.org/docs/reference-manual/>.
- Tierney, L. (1994). Markov chains for exploring posterior distributions. *The Annals of Statistics*, pages 1701–1728.
- Wei, C. H. (2009). Modelling time series of counts with overdispersion. *Statistical Methods and Applications*, 18:507–519.
- Wei, C. H. (2018). *An Introduction to Discrete-Valued Time Series*. John Wiley & Sons.
- Wei, C. H. and Schweer, S. (2015). Detecting overdispersion in inarch(1) processes. *Statistica Neerlandica*, 69(3):281–297.
- Xu, H.-Y., Xie, M., Goh, T. N., and Fu, X. (2012). A model for integer-valued time series with conditional overdispersion. *Computational Statistics & Data Analysis*, 56(12):4229–4242.
- Zhu, F. (2011). A negative binomial integer-valued GARCH model. *Journal of Time Series Analysis*, 32(1):54–67.
- Zhu, F. (2012). Modeling overdispersed or underdispersed count data with generalized Poisson integer-valued GARCH models. *Journal of Mathematical Analysis and Applications*, 389(1):58–71.

## A. Appendix

In this Appendix, we lay out the proofs of [Theorems 2.2](#) and [2.3](#) stated in [Section 2](#) and plots of convergence diagnostics for the Bayesian estimation of parameters in the simulation study conducted in [Section 4](#).

### A.1. Proof of [Theorem 2.2](#)

*Proof.* The proof is influenced by the works of [Fong et al. \(2007\)](#) and [Zhu \(2011\)](#). Assuming first-order stationarity, let

$$\begin{aligned}\gamma_{it} &= \text{Cov}[X_t, X_{t-i}], \\ &= E[X_t X_{t-i}] - E[X_t]E[X_{t-i}], \\ &= E[X_t X_{t-i}] - \mu^2, \quad i = 0, 1, \dots, p.\end{aligned}$$

So, we need only consider  $E[X_t X_{t-i}]$  to derive the conditions as  $\mu^2$  remains a constant. Without loss of generality, we assume  $\mu = 0$ . Additionally, assume  $\mathcal{C}$  to be a constant independent of  $t$ . If the process is second - order stationary, we have

$$\gamma_{jt} = \gamma_{j,t-i}, \quad i = 0, 1, \dots, p, \text{ and } j \in \mathbb{Z},$$

where  $\mathbb{Z} = \{\dots, -1, 0, 1, \dots\}$ . From [\(2.3\)](#), and by definition we arrive at

$$\begin{aligned}E[X_t^2 | \mathcal{F}_{t-1}] &= \text{Var}[X_t | \mathcal{F}_{t-1}] + E^2[X_t | \mathcal{F}_{t-1}] = \lambda_t \left( \frac{1+\phi}{1-\phi} \lambda_t - 1 \right) + \lambda_t^2 \\ &= \alpha_0(\zeta\alpha_0 - 1) + (2\zeta\alpha_0 - 1) \sum_{i=1}^p \alpha_i X_{t-i} + \zeta \left\{ \sum_{i=1}^p \alpha_i^2 X_{t-i}^2 + \sum_{i \neq j}^p \alpha_i \alpha_j X_{t-i} X_{t-j} \right\},\end{aligned}$$

where  $\zeta = \frac{2}{1-\phi}$ . For  $s = 1, \dots, p-1$ , the covariance between  $X_t$  and  $X_{t-s}$  is

$$\begin{aligned}\gamma_{st} &= E[E[X_t | \mathcal{F}_{t-1}] X_{t-s}] \\ &= E[\alpha_0 X_{t-s} + \sum_{i=1}^p \alpha_i X_{t-i} X_{t-s}] = \alpha_0 \mu + \sum_{\substack{i=1 \\ i \neq s}}^p \alpha_i \gamma_{|i-s|,t} + \alpha_s \gamma_{0,t-s} \\ &= \alpha_0 \mu + \alpha_l \gamma_{0,t-s} + \sum_{|i-s|=1} \alpha_i \gamma_{1t} + \dots + \sum_{|i-s|=s} \alpha_i \gamma_{st} + \dots + \sum_{|i-s|=p-1} \alpha_i \gamma_{p-1,t},\end{aligned}$$

where  $\gamma_{j,t-i}$  are replaced by  $\gamma_{j,t}$  for  $i = 1, \dots, p-1$  and  $j \in \mathbb{Z}$ . Hence, for  $s = 1, \dots, p-1$ ,

$$\alpha_0 \mu + \beta_{l0} \gamma_{0,t-s} + \sum_{r=s}^{p-1} \beta_{sr} \gamma_{rt} = 0.$$

Therefore,

$$M(\gamma_{1t}, \dots, \gamma_{p-1,t})^T = -\left(\alpha_0 \mu + \nu_{10} \gamma_{0,t-1}, \dots, \alpha_0 \mu + \nu_{p-1,0} \gamma_{0,t-p+1}\right)^T,$$

then

$$\gamma_{st} = -\alpha_0 \mu \sum_{r=1}^{p-1} m_{sr} - \sum_{r=1}^{p-1} m_{sr} \beta_{r0} \gamma_{0,t-r}, \quad s = 1, \dots, p-1.$$

Let  $\mathcal{C} = \zeta\alpha_0^2 - \alpha_0 + (2\zeta\alpha_0 - 1)\sum_{i=1}^p \alpha_i\mu$ . The unconditional second moment of  $X_t$ ,  $\gamma_{0t} = E[X_t^2]$ , can be rewritten as

$$\begin{aligned}
\gamma_{0t} &= \mathcal{C} + \zeta \left\{ \sum_{u=1}^p \alpha_r^2 \gamma_{0,t-r} + \sum_{i,j=1}^p \alpha_i \alpha_j \gamma_{|i-j|,t} \right\} = \mathcal{C} + \zeta \left\{ \sum_{r=1}^p \alpha_r^2 \gamma_{0,t-r} + \sum_{v=1}^{p-1} \sum_{|i-j|=v} \alpha_i \alpha_j \gamma_{vt} \right\} \\
&= \mathcal{C} + \zeta \left\{ \sum_{r=1}^p \alpha_r^2 \gamma_{0,t-r} + \sum_{v=1}^{p-1} \sum_{|i-j|=v} \alpha_i \alpha_j \left( -\alpha_0 \mu \sum_{u=1}^{p-1} m_{sr} - \sum_{r=1}^{p-1} m_{sr} \nu_{r0} \right) \gamma_{0,t-r} \right\} \\
&= \mathcal{C}_0 + \zeta \left\{ \sum_{r=1}^p \alpha_r^2 \gamma_{0,t-r} - \sum_{r=1}^{p-1} \left( \sum_{v=1}^{p-1} \sum_{|i-j|=v} \alpha_i \alpha_j m_{vr} \nu_{r0} \right) \gamma_{0,t-r} \right\} \\
&= \mathcal{C}_0 + \zeta \left\{ \sum_{r=1}^{p-1} \left( \alpha_r^2 - \sum_{v=1}^{p-1} \sum_{|i-j|=v} \alpha_i \alpha_j m_{vr} \nu_{r0} \right) \gamma_{0,t-r} + \alpha_p^2 \gamma_{0,t-p} \right\},
\end{aligned}$$

or equivalently,

$$\gamma_{0t} = \mathcal{C}_0 + \sum_{r=1}^p L_r \gamma_{0,t-r},$$

where  $L_r = \zeta(\alpha_r^2 - \sum_{v=1}^{p-1} \sum_{|i-j|=v} \alpha_i \alpha_j m_{vr} \nu_{r0})$ ,  $u = 1, \dots, p-1$ ,  $L_p = \zeta\alpha_p^2$  and  $\mathcal{C}_0 = \mathcal{C} - \alpha_0 \mu \sum_{v=1}^{p-1} \alpha_i \alpha_j \sum_{r=1}^{p-1} m_{vr}$ . Therefore, the non-homogeneous difference equation has a stable solution if the equation  $1 - L_1 b^{-1} - \dots - L_p b^{-p} = 0$  has all roots inside the unit circle.  $\square$

### A.2. Proof of [Theorem 2.3](#)

*Proof.* Let  $I_t$  be the  $\sigma$ -field generated by  $\{\lambda_t, \lambda_{t-1}, \dots\}$ , then we have

$$E[X_t | \mathcal{F}_{t-1}, I_t] = E[X_t | \mathcal{F}_{t-1}] = \lambda_t. \quad (\text{A.1})$$

From (2.3), we have  $E[X_t | \mathcal{F}_{t-1}] = \lambda_t$ , and  $Var[X_t | \mathcal{F}_{t-1}] = \lambda_t \left( \frac{1+\phi}{1-\phi} \lambda_t - 1 \right)$ . So, for  $h \geq 0$

$$\begin{aligned}
Cov[X_t - \lambda_t, \lambda_{t-h}] &= E \left[ (X_t - \lambda_t - \underbrace{E[X_t - \lambda_t]}_0) (\lambda_{t-h} - \underbrace{E[\lambda_{t-h}]}_\mu) \right] \\
&= E \left[ (X_t - \lambda_t) (\lambda_{t-h} - \mu) \right] \\
&= E \left[ (\lambda_{t-h} - \mu) E[X_t - \lambda_t | I_t] \right] \\
&= E \left[ (\lambda_{t-h} - \mu) (E[E[X_t | \mathcal{F}_{t-1}, I_t] | I_t] - \lambda_t) \right] \\
&= E \left[ (\lambda_{t-h} - \mu) (E[\lambda_t | I_t] - \lambda_t) \right] = 0.
\end{aligned} \quad (\text{A.2})$$

Similarly, for  $h < 0$ , from (2.2), we have

$$\begin{aligned}
Cov[X_t, X_{t-h} - \lambda_{t-h}] &= E \left[ (X_t - \mu) (X_{t-h} - \lambda_{t-h}) \right] \\
&= E \left[ (X_t - \mu) E[(X_{t-h} - \lambda_{t-h}) | \mathcal{F}_{t-h-1}] \right] \\
&= E \left[ (X_t - \mu) \underbrace{(\lambda_{t-h} - E[\lambda_{t-h} | \mathcal{F}_{t-h-1}])}_0 \right] = 0.
\end{aligned} \quad (\text{A.3})$$

From (A.2) and (A.3), we have

$$\text{Cov}[X_t, \lambda_{t-h}] = \begin{cases} \text{Cov}[\lambda_t, \lambda_{t-h}]; & h \geq 0, \\ \text{Cov}[X_t, X_{t-h}]; & h < 0, \end{cases} \quad (\text{A.4})$$

which is due to the property  $\text{Cov}[X - Y, Z] = \text{Cov}[X, Z] - \text{Cov}[Y, Z]$ . For  $h \geq 0$ , from (2.2) and (A.4), we have

$$\begin{aligned} \gamma_\lambda(h) &= \text{Cov}[\lambda_t, \lambda_{t-h}] \\ &= \sum_{i=1}^p \alpha_i \text{Cov}[X_{t-i}, \lambda_{t-h}] + \sum_{j=1}^q \beta_j \text{Cov}[\lambda_{t-j}, \lambda_{t-h}] \\ &= \sum_{i=1}^{\min(h,p)} \alpha_i \text{Cov}[\lambda_{t-i}, \lambda_{t-h}] + \sum_{i=h+1}^p \alpha_i \text{Cov}[X_{t-i}, X_{t-h}] + \sum_{j=1}^q \beta_j \text{Cov}[\lambda_{t-j}, \lambda_{t-h}]. \end{aligned} \quad (\text{A.5})$$

Similarly, for  $h \geq 1$ , we have

$$\begin{aligned} \gamma_X(h) &= \text{Cov}[X_t, X_{t-h}] \\ &= \text{Cov}[\lambda_t, X_{t-h}] \\ &= \sum_{i=1}^p \alpha_i \text{Cov}[X_{t-i}, X_{t-h}] + \sum_{j=1}^q \beta_j \text{Cov}[\lambda_{t-j}, X_{t-h}] \\ &= \sum_{i=1}^p \alpha_i \text{Cov}[X_{t-i}, X_{t-h}] + \sum_{j=1}^{\min(h-1,q)} \beta_j \text{Cov}[X_{t-j}, X_{t-h}] + \sum_{j=h}^q \beta_j \text{Cov}[\lambda_{t-j}, \lambda_{t-h}]. \end{aligned} \quad (\text{A.6})$$

□

### A.3. Plots from the Simulation study

#### A.3.1. Histograms of posterior distributions, traceplots and autocorrelation of parameters for NoGe-INARCH(1) model

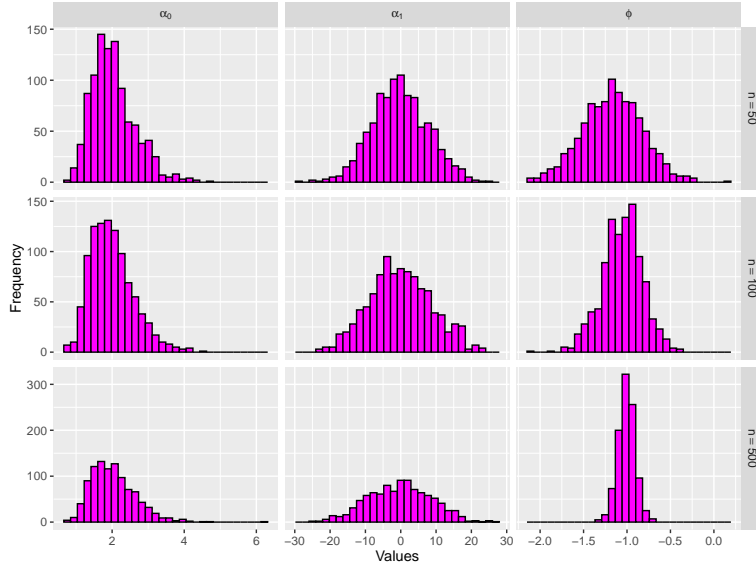


Figure 7: Histograms of posterior distributions for parameters,  $\alpha_0$ ,  $\alpha_1$  and  $\phi$  for various sample sizes of NoGe -INARCH(1) model.

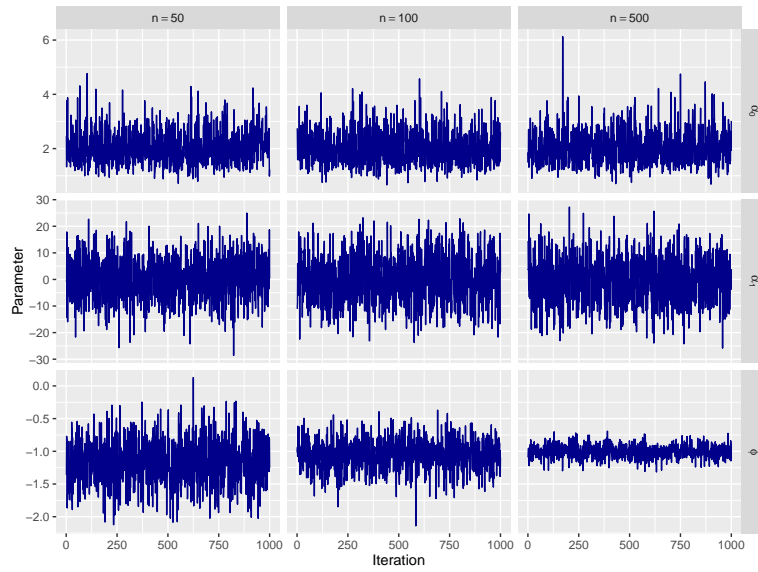


Figure 8: Traceplots for parameters,  $\alpha_0$ ,  $\alpha_1$  and  $\phi$  for various sample sizes of NoGe -INARCH(1) model.

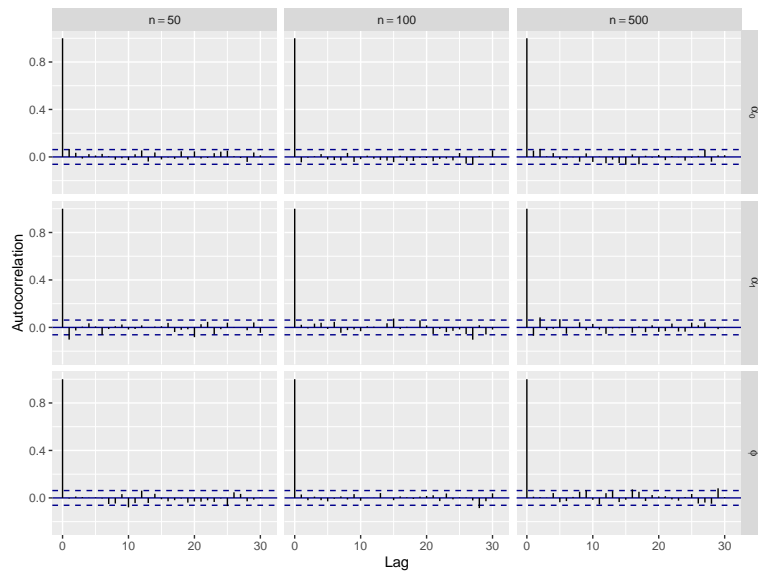


Figure 9: Autocorrelation for parameters,  $\alpha_0$ ,  $\alpha_1$  and  $\phi$  for various sample sizes of NoGe -INARCH(1) model.

NOTE: The plots are presented for the case of transformed unconstrained parameters. That is, since some of the parameters are constrained, as mentioned in [Subsection 3.1](#), we have applied logit transformation for them to vary along the real line. For example, in the case of INARCH(1) model where  $\phi = 0.3$  is bounded between 0 and 1, after applying the transformation, the unconstrained parameter has the value -0.85.

A.3.2. Histograms of posterior distributions, traceplots and autocorrelation of parameters for NoGe-INARCH(2) model

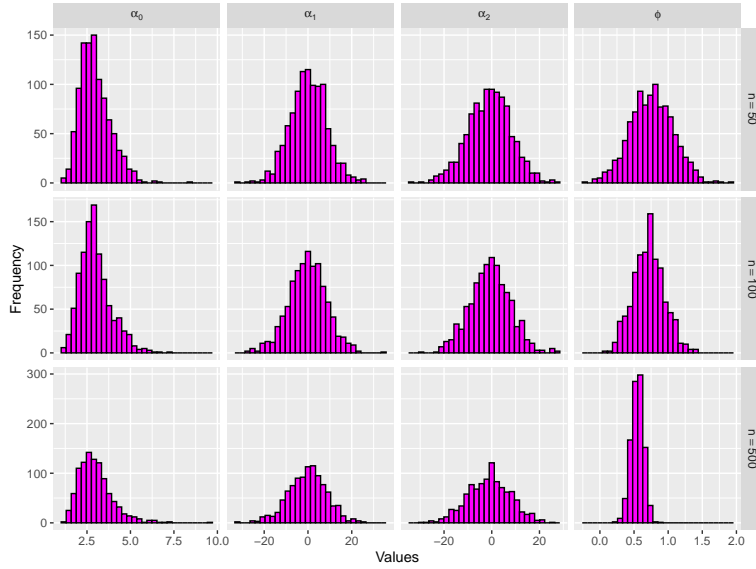


Figure 10: Histograms of posterior distributions for parameters,  $\alpha_0$ ,  $\alpha_1$ ,  $\alpha_2$  and  $\phi$  for various sample sizes of NoGe -INARCH(2) model.

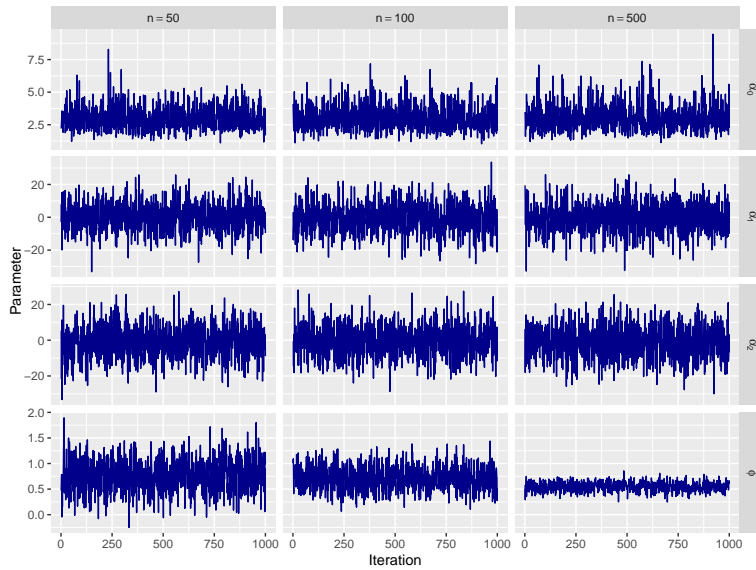


Figure 11: Traceplots for parameters,  $\alpha_0$ ,  $\alpha_1$ ,  $\alpha_2$  and  $\phi$  for various sample sizes of NoGe -INARCH(2) model.

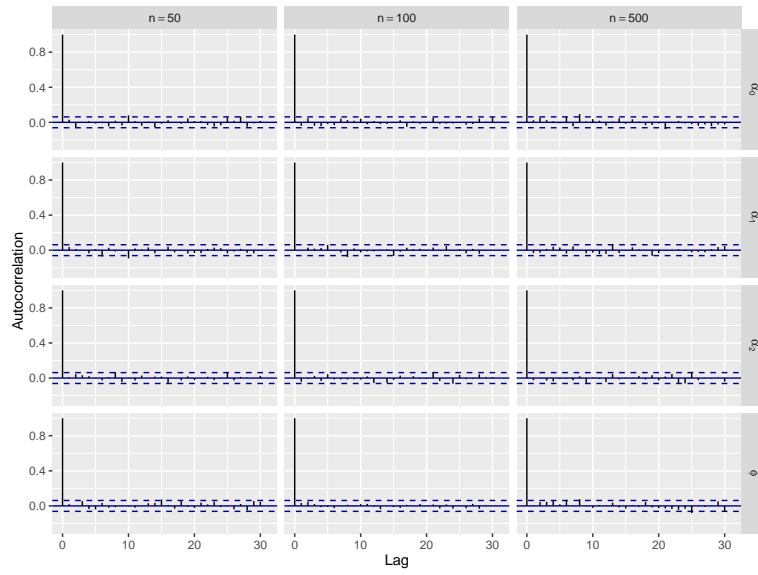


Figure 12: Autocorrelation for parameters,  $\alpha_0$ ,  $\alpha_1$ ,  $\alpha_2$  and  $\phi$  for various sample sizes of NoGe -INARCH(2) model.

*A.3.3. Histograms of posterior distributions, traceplots and autocorrelation of parameters for NoGe-INGARCH(1,1) model*

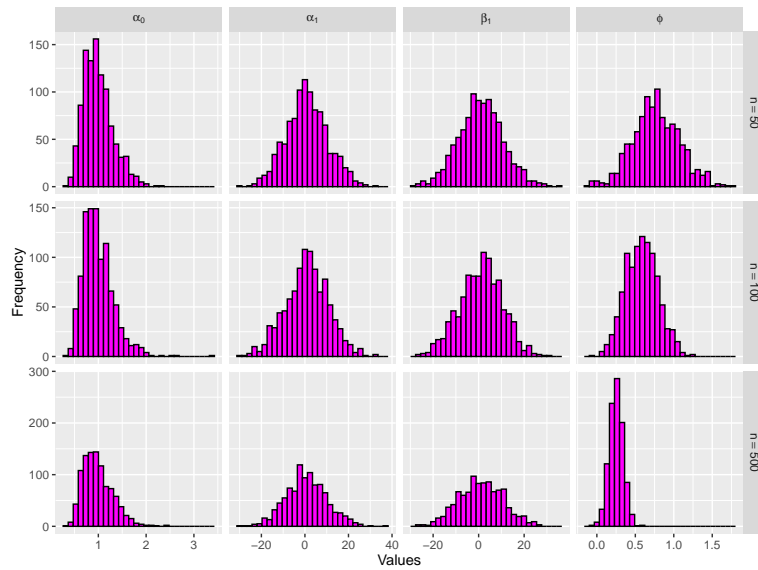


Figure 13: Histograms of posterior distributions for parameters,  $\alpha_0$ ,  $\alpha_1$ ,  $\beta_1$  and  $\phi$  for various sample sizes of NoGe -INGARCH(1,1) model.



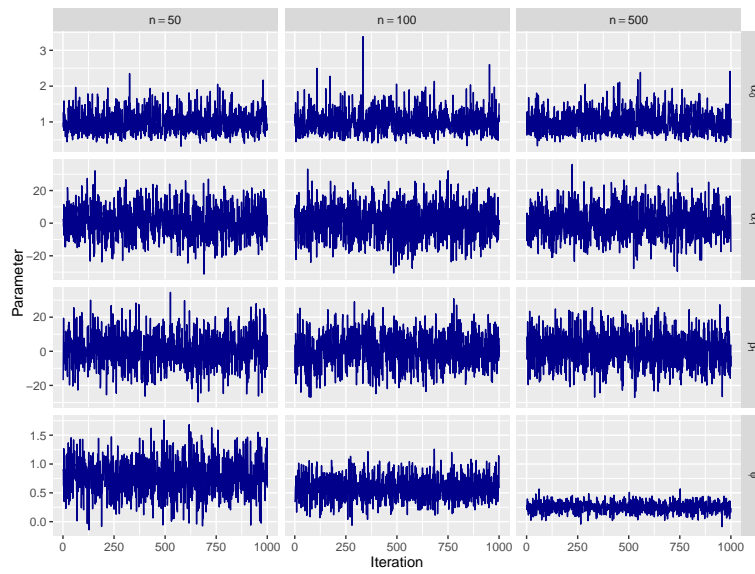


Figure 14: Traceplots for parameters,  $\alpha_0$ ,  $\alpha_1$ ,  $\beta_1$  and  $\phi$  for various sample sizes of NoGe - INGARCH(1,1) model.

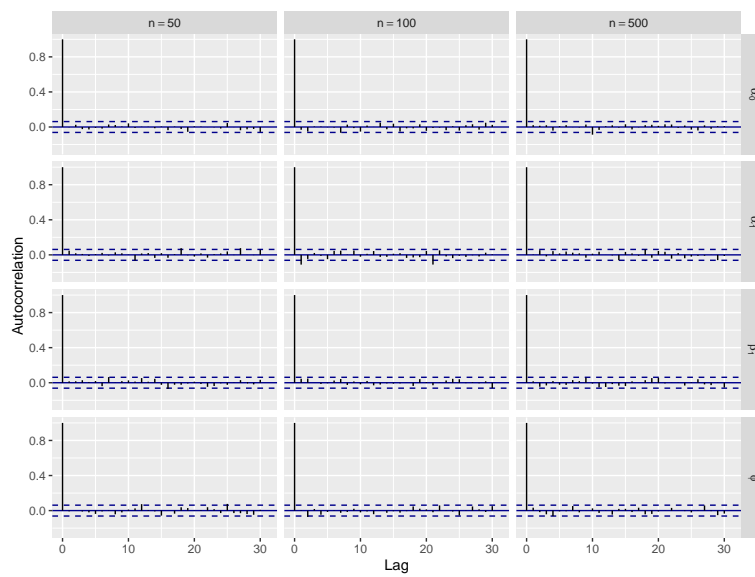


Figure 15: Autocorrelation for parameters,  $\alpha_0$ ,  $\alpha_1$ ,  $\beta_1$  and  $\phi$  for various sample sizes of NoGe - INGARCH(1,1) model.